# Magnetic Determination of Average Catalyst Temperatures in Fluidized Beds

**Timothy S. Cale and J. A. Merson**
Dept. of Chemical, Bio & Materials Engineering and Center for Energy Systems Research, Arizona State University, Tempe, AZ 85287

*A magnetic method to measure the time and spatial average temperature of supported nickel catalysts in fluidized beds is detailed. It is an extension of a magnetic method developed in this laboratory to study fixed beds. The RMS output voltage of an AC permeameter is used to follow changes in the magnetic moment, hence temperature, of the catalyst upon starting or stopping ethane hydrogenolysis. The theory of the thermometry in fluidized beds is detailed and the observed RMS output voltage vs. time traces for typical experiments are explained. Simulations indicate that signals generated by the moving particles are largely averaged out, since the direction of the magnetic moment of each catalyst particle follows the applied field and is independent of movement. Filtering in the frequency domain can be used to further reduce the effects of particle movement. Calibrations needed to convert AC permeameter output voltage changes to changes in sample temperature during experiments on two distinctly different fluidized beds are the same as for the respective fixed beds. Depending somewhat on the sample moment, the average solid temperature can be determined with a repeatability of a few tenths of a degree.*

## Introduction

Catalyst temperature is of fundamental importance in heterogeneous catalytic reactors; unfortunately, few experimental techniques of general use are available for its measurement. The local catalyst and fluid temperatures are close in typical industrial fixed-bed reactors so there usually is not much motivation to measure catalyst temperature. In situations where large catalyst particles are used and their temperatures are desired, they are measured using thermocouples in individual catalyst particles. On the other hand, interphase transport and kinetic experiments indicate that the catalyst and fluid temperatures can differ significantly in low Reynolds number (Re) flows common in fluidized beds and laboratory fixed beds (Hudgins, 1981; Cale, 1984; Cale and Lawson, 1985). This is particularly true for fluidized beds, the focus of this article, because the choice of this mode of operation is often based on the high sensible heat generation associated with the reaction to be run. The very small catalyst particle sizes and the particle movement found in these systems combine to interfere with solid temperature measurements.

Correspondence concerning this article should be addressed to T. S. Cale.

Techniques for measuring the temperature of fluidized solids have been reviewed (Stubington, 1985; Geldart, 1986). Individual particle temperatures can be obtained fairly reproducibly using thermocouples attached to fixed or oscillating particles (Stubington, 1985). Several groups have used suction probes to sample solid particles and measure their temperatures (Geldart, 1986); however, the measured temperature depends on the suction pressure drop. A more noninvasive method is the use of fusible material in carefully designed solid particles. The state of the material after bed operation indicates whether or not the particle reached the temperature required for fusion. This method provides very limited resolution. In addition, the interpretations of the temperatures determined by these methods are uncertain since the sampled or tagged solid particles may not be representative of the bed. For example, the effect of conduction along a thermocouple attached to a very small particle is difficult to quantify. When applicable, optical methods provide measures of solid temperatures near a surface or boundary of the bed (Stubington, 1985). Again, the solids at a boundary of a bed may not be representative of the solids in the bed. In addition, these methods are plagued by cali-

bration uncertainties. The temperatures measured by shielded and bare thermocouples in fluidized beds have been compared and the latter are recommended by Grace and Baeyens (Geldart, 1986). Some ill-defined average of solid and fluid phase temperatures is measured by this approach; therefore, the solid temperature is only measured well if the temperature difference between the phases is small. In summary, there is no widely accepted method to measure a "representative" solid temperature in fluidized beds.

This article introduces a method to measure the volume average temperature of magnetic solids in a fluidized bed. Although the experimental arrangement used in this laboratory is discussed along with some representative results, the emphasis is on the theory behind the thermometry and the interpretation of experimental data. These should be applicable to other experimental configurations. The thermometry provides a representative solid temperature of particular interest for the study of fluidized beds, because spatial uniformity of solid temperature is a common assumption used in their modeling. Thus, the method provides information previously unobtainable and is applicable whether or not there are temperature differences between the catalyst particles and the fluid. In addition, the magnetic thermometry has the distinct advantage that it is not invasive, because the sensing coils are outside of the reactor. No bed stabilization due to the magnetic field is expected for this system, since the magnetic moment of the catalyst is much lower than typically used in such systems (Rosensweig, 1985; Arnaldos et al., 1987). In addition, the applied field is on the order of only 100 Gauss at 47 Hz. This method is an extension of the magnetic thermometry developed to measure the volume average catalyst temperature in fixed beds of superparamagnetic nickel catalysts during ethane hydrogenolysis (Cale, 1984; Cale and Ludlow, 1984a).

The volume average temperature determined is that of the supported nickel crystallites. However, the fixed-bed magnetic thermometry has provided clear evidence that the time-average temperature of the nickel crystallites is the same as that of the surrounding support. This is expected for reactions with reasonable parameters (Luss, 1970; Holstein and Boudart, 1983) and should be valid for most catalytic reaction systems. In particular, it does not depend on the catalyst's state of fluidization. Thus, the magnetically determined volume average temperature is also the volume average catalyst temperature. The fixed-bed magnetic thermometry provides a previously unavailable measure of average solid temperature which has been used in parameter estimation for several fixed-bed reactor models (Cale et al., 1987) and to determine interphase heat-transfer coefficients within the differential reactor assumption (Cale and Lawson, 1985). The behavior of single catalyst pellets has also been studied (Cale, 1988). The magnetic thermometry has also been extended to determine the cross-sectional axial temperature profile in a packed bed reactor (Cale and Merson,1989). Though currently limited experimentally to supported nickel catalysts, model developments resulting from these catalyst temperature measurements will in general apply to other heterogeneous catalytic systems.

## Experimental Studies

The basis of the thermometry used in this work is the temperature dependence of the magnetic moment density, or intrinsic magnetization, of supported nickel catalytic crystallites (Cale, 1984). The catalyst temperature is changed by starting and stopping ethane hydrogenolysis, and the thermometry is performed during both types of experiments. This cycling is done by starting and stopping ethane flow in a stream containing hydrogen and helium. The change in temperature is determined by the difference in steady-state sample magnetic moments before and after reaction initiation or termination. The change in moment density, hence sample temperature, can be determined for superparamagnetic samples using low magnetic field intensities. For the thermometry, the output voltage of an AC permeameter (ACP) is used to follow changes in the magnetic moment of the catalyst (Selwood, 1975). Only changes in temperature are studied in order to avoid the need for absolute values of moment density, which would be very difficult to determine using an ACP. The axis of the ACP used in this work is vertical and the upper secondary coil is used to sense changes in sample moment (Cale and Merson, 1989; Cale and Ludlow, 1984b). The RMS output voltage increases in response to the introduction of superparamagnetic samples. The catalyst bed is centered in this secondary, in the absence of flow, for measurements. The excitation frequency is 47 Hz, with a primary current of about 200 mA, yielding field strengths on the order of 100 Gauss. Because this excitation is used in every experiment, precise knowledge of the field strength is not needed as long as the Langevin low field approximation is valid (Cale, 1984; Selwood, 1975).

Two different fluidized catalyst beds have been studied to demonstrate the thermometry. The beds were first used in fixed-bed heat-transfer experiments and the catalysts are well studied (Cale et al., 1987; Ludlow, 1986). They both are 23% nickel on silica catalysts. Catalyst sample A has an average particle size of 0.016 cm. It is packed in a 0.6 cm diameter (ID) reactor to a depth of 2.1 cm. The catalyst of sample B is 0.011 cm in average diameter packed in a 1.1 cm diameter (ID) reactor to a depth of 0.7 cm. The particle sizes given are the arithmetic average of the openings of the sieves used to obtain each catalyst sample. The two reactors used are quartz for inertness and have been thoroughly discussed (Cale, 1984; Cale and Ludlow, 1984b). A fritted quartz disk serves as the distributor in each reactor. The inlet thermocouple is in a well just below this disk in each reactor. The outlet thermocouple well is placed 1 mm above the smoothly fluidized bed in system B. It is 3 mm above the top of the smoothly fluidized bed of system A. The inlet pressure used is just that required for flow. The majority of the small pressure drops observed are due to the quartz frits. Flow maldistribution was apparent during some experiments on system B; however, this does not interfere with the thermometry experiments. The temperature range of the experiments reported is 510–520 K. The ranges of linear velocity are 0.5 to 8 cm/s for bed A and 0.8 to 8 cm/s for bed B. Conversions are kept below 2% in order to be consistent with a fairly arbitrary criterion for differential reactor behavior adopted in this laboratory (Cale and Lawson, 1985). The conversion in each experiment is determined using the flame ionization detector of a Carle AGC, series 400 gas chromatograph.

ACP voltages and thermocouple determined fluid temperatures are logged every 2.2 seconds over an IEEE-488 interface from the measuring voltmeters. A Keithley Model 192, 6.5 place digital multimeter (DMM) is used to measure the ACP

output voltage. The integration period is 100 ms, and the value recorded is the result of averaging six of these integrations. Thus, the voltage recorded is not the average over a continuous time interval. It is essentially the average RMS voltage over the last 0.6 s of the 2.2 s logging interval. The ACP voltage is zeroed before the initiation or termination of reaction (ethane flow), so a decrease in the RMS output of the ACP is recorded as a negative voltage. A Keithley Model 195A, 5.5 place DMM measures the DC voltages from the Type E thermocouples used to determine inlet and outlet fluid temperatures. The fluid temperatures are determined from calibrations provided for the thermocouple input card of a Keithley Model 705 scanner. The temperatures recorded are time averages over part of the logging interval, as described for the ACP voltage.

The *change* in ACP voltage is converted to a *change* in average solid temperature using two calibrations established for each sample for a particular set of operating conditions:

1. A calibration between sample temperature and ACP voltage;
2. A calibration between hydrogen partial pressure and ACP voltage at constant temperature. These calibrations are determined for each catalyst sample before thermometric experiments are started. The calibrations between voltage and temperature are essentially linear over the limited temperature ranges considered in the thermometry experiments, which is usually less than 20 K. Because only changes in temperature are considered, the calibration is essentially a single conversion factor. The no reaction condition provides the reference temperature for both reaction initiation and termination experiments. This reference is chosen since the solid temperature is the same as the gas temperature and the bed is isothermal. The ACP/reactor has been verified to be isothermal to within thermocouple reproducibility ($\pm 0.1$ K) over more than 4 cm axially, which is much longer than either bed considered in this work. The thermocouples used to measure the inlet and outlet fluid temperatures indicate an apparent difference of 0.6 K at reaction temperatures due to their limited accuracy. The temperature indicated by the thermocouple at the bed outlet is used as the reference; that is, the value indicated by the inlet thermocouple is adjusted to read the same temperature in the no reaction state. As only changes in temperature are followed, this serves to completely define the reference temperature. Over the limited range of temperature seen during a typical thermometry experiment (a few degrees), the temperature sensitivities of the two thermocouples are assumed equal. The changes in temperature are added to the reference value to obtain absolute temperatures.

The magnetochemistry of the reaction system is an interference to the thermometry. The magnetic moment of the nickel, hence the sample, is affected by the extent of surface coverage by hydrogen (Selwood, 1975). It decreases with increasing coverage or partial pressure of hydrogen over the nickel. One of the principal reasons that ethane hydrogenolysis is used in the thermometry is that ethane does not affect the moment of nickel in the presence of hydrogen (Cale, 1984). This has been verified experimentally, up to temperatures where significant reaction occurs (Ludlow, 1986). This is assumed to be true at reaction temperatures also, which is supported by the rate form (Cale, 1984). The interference occurs because the partial pressure of hydrogen decreases upon the introduction of ethane. This causes the sample moment to increase due to desorption of hydrogen (Selwood, 1975). This increase opposes the decrease caused by the increase in catalyst temperature upon reaction initiation and the observed decrease must be increased in magnitude. Similarly, the increase in voltage observed upon reaction termination must also be increased in magnitude.

This interference is accounted for by determining the relationship between ACP voltage and the partial pressure of hydrogen (Cale, 1984). If the negative of the change in ACP voltage is plotted against hydrogen partial pressure, the result is essentially an adsorption isotherm (Selwood, 1975). The correction due to this interference is usually only a few percent of the temperature change. This minimizes the impact of the assumption that ethane does not affect the sample moment in the presence of hydrogen at reaction temperatures. The calibration between hydrogen partial pressure and ACP output voltage is determined by changing the partial pressure of hydrogen in a stream of hydrogen and helium. The partial pressure of hydrogen in the bed is assumed uniform during these experiments. The "magnetoadsorption" isotherm is determined at one temperature in the range or interest. It is used over the limited temperature range of the experiments. Changes in uptake with temperature are small relative to the uptake and the total effect of the hydrogen coverage on the thermometry is only a few percent of the moment change. Ignoring the change in uptake of hydrogen with temperature has had no apparent impact in fixed- or fluidized-bed thermometry experiments to date.

Both the temperature-ACP voltage calibration and adsorption isotherm are determined after the catalyst sample has been "aged" by using it for ethane hydrogenolysis. The sample is aged until the magnetic properties of the sample are essentially constant in time. Both calibrations are then fairly constant in time; however, they are routinely checked since they would be affected by catalyst poisoning.

Visual verification of flow regime and bed height measurements were performed by pulling the bed out of the oven and making rapid observations. The measured bed heights seem to be fairly accurate and no qualitative changes in bed behavior due to cooling have been noticed during these extractions.

Finally, there was no significant loss of catalyst during the experiments reported. This would be detected magnetically, as even a 0.1% change in sample moment can be easily detected.

## Theory

The primary conceptual hindrance to applying the magnetic thermometry to fluidized beds is the very movement of the catalyst particles; that is, movement of magnetic particles in sensing coils generates signals. In general, signals generated by moving magnets are large in comparison with signals we observe due to changes in sample temperature and surface coverage. This would inhibit the application of the magnetic thermometry to fluidized beds. The feasibility of the magnetic thermometry is explained in the following paragraphs.

A detailed derivation of the ACP output voltage response to superparamagnetic samples has been presented in the literature (Cale and Merson, 1989). That derivation considers the coil position and time dependence of the ACP output voltage. In this work, the reactor remains at a fixed position in the ACP coils and thus the coil position dependence is not

explicitly considered in the following derivation. Additional complications due to the motion of the particles are discussed below. Using Faraday's law, it can be shown that the instantaneous voltage induced in the sensing secondary coil of the ACP due to the magnetization (moment/volume) of the catalyst sample is the integral of the local rate of change in magnetization times local coil sensitivity (Cale and Merson, 1989):

$$E(t) = \int_0^L \sigma(\xi) \frac{\partial M(\xi, t)}{\partial t} d\xi \tag{1}$$

where $\sigma(\xi)$ is the output voltage of the (entire) ACP per unit rate of change in magnetization at position $\xi$ in the ACP. It is assumed to be uniform radially. Due to the axial symmetry of the coils, the extraction of radial information is not attempted. The interface between the quartz frit and the bed is defined as $\xi = 0$. The length of the catalyst bed $L$ is taken as a constant large enough to encompass all fluidized material. The changes in the magnitude of the local magnetization can be due to changes in amount of magnetic material or changes in the magnetization of a constant amount of material. For the thermometry, we are concerned with the magnitude of the local magnetization.

The Langevin low field approximation for the magnetization of a superparamagnetic specimen (Selwood, 1975) is:

$$M(H, T) = \frac{M_\infty(T) I_S(T) < v > H}{3kT} \tag{2}$$

where $H$ is the magnetic field intensity, $I_S(T)$ is the intrinsic magnetization of the nickel at temperature $T$, $M_\infty(T)$ is the maximum or saturation magnetization of the sample at temperature $T$, $k$ is Boltzmann's constant, and $< v >$ is the average volume of the nickel crystallites. Although the temperature and field may vary in time and/or space, the average crystallite volume is constant on a macroscopic scale. Based on the decrease in magnetic moment upon exposure to hydrogen for the catalyst samples used in this work, an average crystallite radius of 5 nm is a reasonable upper bound for the catalyst samples of this work. Using this number and assuming a uniform distribution of nickel on the silica, there are well over ten million crystallites in each cubic micron of catalyst. Thus, an averaging volume on the order of a cubic micron is sufficient to define the average properties of the catalyst and be small on the scale of a catalyst particle. Note that Eq. 2 applies locally to any such averaging volume in each catalyst particle. The local sample saturation magnetization is the local intrinsic magnetization times the fraction of the cross section occupied by nickel. This is expressed as:

$$M_\infty(T(\xi, t)) = I_S(T(\xi, t))\ \psi\phi(\xi, t) \tag{3}$$

where $\phi$ is the local solid fraction and $\psi$ is volume fraction of solid which is nickel. The latter is on the order of 2% and is uniform on a macroscopic scale. In words, the saturation magnetization is the magnetization which would occur if the moment of every crystallite in the local sample were perfectly aligned with the applied field. This happens only at very high magnetic field intensities, particularly at the temperatures of concern in this work. Thus, the local magnetization at low field intensity is:

$$M(\xi, t) = \left(\frac{I_S^2(T) < v > \psi}{3kt}\right) \phi(\xi, t)\ H(\xi, t) \tag{4}$$

By introducing the dimensionless quantity

$$\Gamma(\xi, t) = \frac{I_S^2(T) < v > \psi}{3kt} \tag{5}$$

to represent the temperature dependence of the local sample magnetization, Eq. 1 can be written as:

$$E(t) = \int_0^L \sigma(\xi) \left[ H(\xi, t) \left[ \phi \frac{\partial \Gamma}{\partial t} + \Gamma \frac{\partial \phi}{\partial t} \right] + \Gamma(\xi, t) \phi(\xi, t) \frac{\partial H}{\partial t} \right] d\xi \tag{6}$$

where the effects of transients in temperature ($\Gamma$), solids fraction and magnetic field have been displayed separately.

The behavior of superparamagnetic samples in an AC field can be explained using Eq. 6. For these samples, the net moment of each catalyst particle (and the entire sample) is very small at the low fields used and follows the applied field. If the applied field is assumed spatially uniform within the sensing secondary coil region and is written as

$$H(t) = H_0 \sin(2\pi f t) = H_0 \sin(\omega t) \tag{7}$$

then Eq. 6 can be written

$$E(t) = H_0 \int_0^L \sigma(\xi) \times \left[ \phi \sin(\omega t) \frac{\partial \Gamma}{\partial t} + \Gamma \sin(\omega t) \frac{\partial \phi}{\partial t} + \Gamma \phi \omega \cos(\omega t) \right] d\xi \tag{8}$$

I II III

The first two terms in the brackets of the integrand in Eq. 8 (term I and term II) are the voltages generated by changes in temperature or the amount of material at $\xi$, respectively. The third term (term III) tracks the temperature and the amount of material at $\xi$. As pointed out in the Experimental Studies section, the RMS voltage is measured relative to some reference voltage. This reference voltage is the time average of the recorded RMS voltage before the thermometry experiment is started. From Eq. 8, the voltage recorded at $t = t_i$ is

$$V(t_i) = < RMS[E(t)] >_i - E_{\text{ref}} \tag{9}$$

As noted, the averaging indicated in Eq. 9 is not a continuous time average, but rather the average over the last 0.6 s of the 2.2-s logging interval.

The interpretations of the experimental results presented in the following paragraphs are validated by computer simulations. Equation 9 was used to compute the time trace of the ACP voltage which would be recorded using the experimental

configuration described in the Experimental Studies section for several different assumptions regarding the time and spatial dependencies of $\Gamma(\xi, t)$, $\phi(\xi, t)$ and $\sigma(\xi)$ in the integral of Eq. 8. Typical simulations modeled temperature changes by first-order responses and assumed temperature to be spatially uniform.

Particle motion was modeled using sinusoidally oscillating beds. The bed height was assumed to oscillate by as much as a factor of two at distinct as well as mixed frequencies of less than 10 Hz. Several frequencies and frequency combinations were used. The model is not intended to provide an accurate description of the bed motion; however, it provides insight to the voltage vs. time traces obtained experimentally. In particular, conclusions drawn from the simulations should be valid for any fluidization pattern which can be represented by a Fourier series, as long as the majority of the bed movement is at frequencies of less than 10 Hz. The coil sensitivity was assumed spatially uniform for the simulations, because this is the case for the experimental results reported.

The results of these simulations indicate that term I is much smaller than either of the other terms for any realistic rate of temperature change. It can be ignored. Term II represents the major conceptual difficulty with performing the magnetic thermometry on fluidized beds. Fortunately, the moment vector (field vector) of each particle is not correlated with its movement. Note that the orientation of a catalyst particle is of no concern, since the moment of each crystallite in the particle is mobile. Since the frequency of excitation is 47 Hz, the direction of the net moment reverses itself several times over the upward or downward movement of each catalyst particle. Thus, the voltage generated by movement in any direction changes sign several times over a particles' movement and largely averages out for each particle. The positive and negative voltages generated by the movement of each particle might not exactly cancel out, since the particle will change velocity and reverse direction. A small net voltage might be generated because of this velocity change, depending on the timing of the change relative to the moment vector and the DMMs integration cycle.

Additional averaging occurs for particles moving in an uncorrelated manner and the majority of the signal generated which might be caused by the movement of individual particles (as discussed in the previous paragraph) is averaged out. On the other hand, aggregative movements, such as slugging or the expansion of the bed due to increased flow might be detected. The direction and extent of the change in voltage depends on the extent, speed, and timing of the expansion or slug relative to the field and voltmeter integration cycle. The RMS voltages generated due to term II in the case of aggregative particle movements can be significant relative to the changes in voltage which are used to measure temperature changes (term III in Eq. 8). These latter changes are on the order of 1%. The simulations indicate that the voltages generated by particle movement can be removed by (fast) Fourier transforming the data, filtering in the frequency domain, and then back-calculating the time trace. If filtering is used, the effects of term II are reduced significantly. Thus, signals due to term III of Eq. 8 can be isolated and used for the thermometry, as for fixed beds (Cale and Merson, 1989).

## Results and Discussion

The discussion in the previous paragraphs explains the voltage vs. time traces observed in the thermometry experiments. At low flows, both beds used in the experiments of this work are smoothly fluidized (Kunii and Levenspiel, 1969; Geldart, 1986) and the fluctuations of the surfaces are on the order of a few Hz, with amplitudes of about 1 mm. The particles of the bed are not moving in a concerted manner. Rather, they are moving essentially randomly relative to each other on the scale of the bed. This inherent averaging, along with the averaging of the voltmeter, averages out the majority of the signal generated by particle movement. Figure 1a shows a time trace of the ACP voltage upon starting ethane hydrogenolysis for system A in the smoothly fluidized regime. With the exception of the "spike" upon increasing the flow, the signal vs. time trace for the smoothly fluidized system is much like that for fixed beds (Cale, 1984). Such a transient occurs occasionally, and is apparently the result of a large temporary bed expansion caused by excessive pressure initially behind the valve downstream of the ethane mass flow controller. The decrease in voltage due to initiation of ethane hydrogenolysis is observed to be 30 $\mu$V. It is simply the difference between the initial and final baselines. The noise level is several microvolts, as in the fixed-bed thermometry.

At higher flows the bed becomes aggregated for system A, while system B appears to be smoothly fluidized over the range of linear velocities studied. This is consistent with the discussions of Kunii and Levenspiel (1969) as well as Geldart (1986), for such systems. All voltage vs. time results from system B had much the same signal-to-noise level as in Figure 1a. No attempt to discern between bubbling and slugging in system A is made, and the term slugging is used because of the small reactor diameter. The transition to aggregated flow is taken to be when the top of the bed begins substantial, pulsing vertical motion. These slugs occur at much lower frequency than the oscillation of the bed surface observed in the smoothly fluidized systems. They also take a significant amount of time. More importantly, voltage excursions are measured at apparently random times in the aggregated flow regime. Time traces of AC permeameter output voltage for system A during thermometry experiments in the aggregated flow regime are shown in Figures 1b and 1c. Both represent experiments where hydrogenolysis was started. From these figures, there seems to be two different kinds of spikes; one kind occurs in both positive and negative directions and are on the order of 20 to 30 $\mu$V, while the other kind is always negative and is usually larger than 50 $\mu$V.

The smaller spikes can be explained as due to slugs passing through the bed and represent the effect of term II of Eq. 8. As noted above, the signal generated by movement is largely averaged out for each particle. In the case of aggregative solids movement, the particles move in a more correlated manner than in smoothly fluidized beds. Thus, the averaging process due to random particle motion is not as pronounced as in smoothly fluidized beds. The direction and extent of change in RMS voltage depends on the aggregative solids movement relative to the excitation voltage vector and voltmeter integration cycle. The larger, negative spikes are apparently due to significant amounts of catalyst being in less sensitive regions of the sensing secondary coil over the integration period of the DMM. Less catalyst is in the maximum sensitivity region of the coil, and a negative spike occurs. This term results from term III of Eq. 8. The higher the flow rate, the more frequent

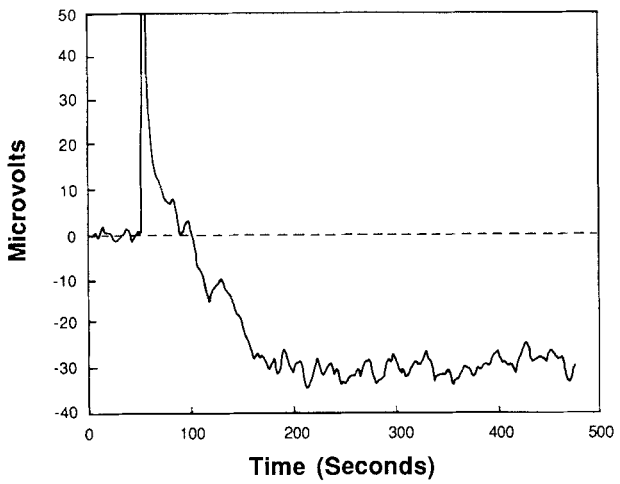


**Figure 1a. Voltage trace for a smoothly fluidized bed.**

these spikes; however, a definite baseline is present or the thermometry is not performed. Thus, the ACP output voltage trace is essentially the same as that observed in the smoothly fluidized- and fixed-bed modes, except for a series of spikes. The trace in Figure 1c represents the upper limit of solids movement over which thermometry has been performed. Even in this case, the decrease in voltage over time can be determined to within a few microvolts. The smooth curve in Figure 1c, below the time trace is the result of Fourier transforming (FFT) the data, filtering in the frequency domain and recomputing the time trace. The offset was introduced to allow the curve to be seen. The voltage changes in time between the steady state values probably reflect changes in hydrogen coverage and average catalyst temperature as the reaction starts. Only the initial and final baselines are currently used in the thermometry. As mentioned, thermometry has not been attempted at higher flows than in the run of Figure 1c, both for the reason cited and because of bed expansion effects discussed in the following paragraphs. The calibrations for temperature and hydrogen coverage have been experimentally verified to be quantitatively the same in both smoothly fluidized and slugging bed modes, over the flow range studied, as in fixed beds.

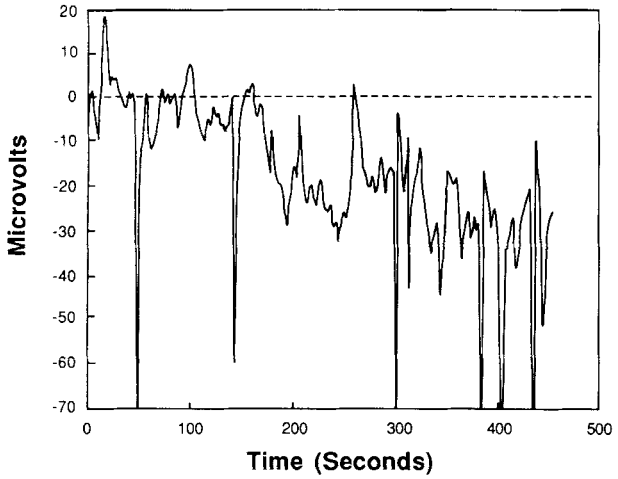


**Figure 1b. Voltage trace for a slugging bed.**

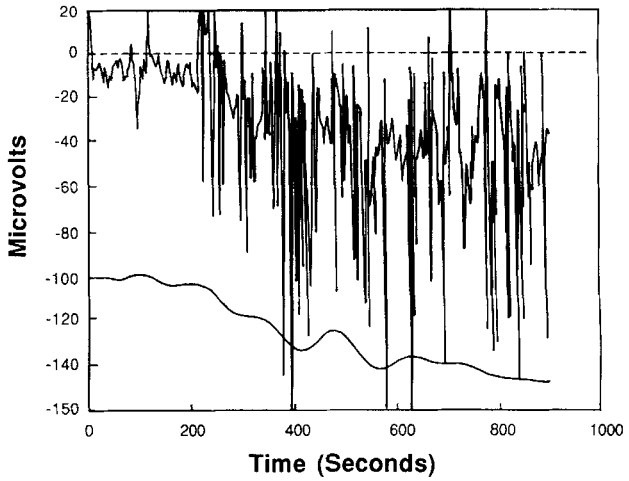


**Figure 1c. Original and smoothed voltage traces for a more vigorously slugging bed (compared to b).**

All data are from experiments where ethane hydrogenolysis is started on system A.

If sensing coil end effects are not important, so that the ACP sensitivity is spatially uniform, then the expansion of the bed upon starting ethane flow will have no lasting impact on output voltage. The local value of $\phi$ in term III of Eq. 8 is balanced by the increase in length over which there is material. Thus, the voltage returns to the previous baseline, even if the expansion is detected (as a slug might be) due to term II. If coil sensitivity end effects are important, the RMS voltage decreases as the bed approaches the top of the sensing coil as a result of increased flow. This is due to the decrease in sensitivity of the sensing secondary coil towards its ends. For example, the ratio of bed length to sample coil length is 0.42 for the 2.1-cm-long bed (A), and such end effects are found for bed height increases of about 15%. This estimate of bed height increase is based on measurements made upon pulling the reactor out of the coils, as discussed in the Experimental Studies section. More importantly, the steady state shift in baseline voltage due to expansion is related to helium flow rate for system A, as shown in Figure 2. There is no noticeable change in baseline until about 60 std. mL/min of helium flows through the bed, corresponding to the 15% bed height increase. A hysteresis is also observed. Upon contraction of an expanded bed, the flow has to be lower to reestablish a given voltage level. For the shorter bed (system B), no end effects were discerned in the flow range used.

Any change in voltage due to bed expansion or contraction upon initiating or stopping ethane flow occurs very rapidly on the time scale of the thermometry experiments. Thus, it is easily distinguished from the changes due to concentration changes as the ethane reaches the bed. These changes include the initiation of ethane hydrogenolysis as well as the effects of changes in hydrogen partial pressure. Any further changes in bed height due to changes in gas density would be difficult to separate from the effect of temperature, but should be small for this gas-solid system (Kunii and Levenspiel, 1969; Geldart, 1986). Nevertheless, thermometry has not been attempted in this flow regime. For systems such as B of this study, there is no reason

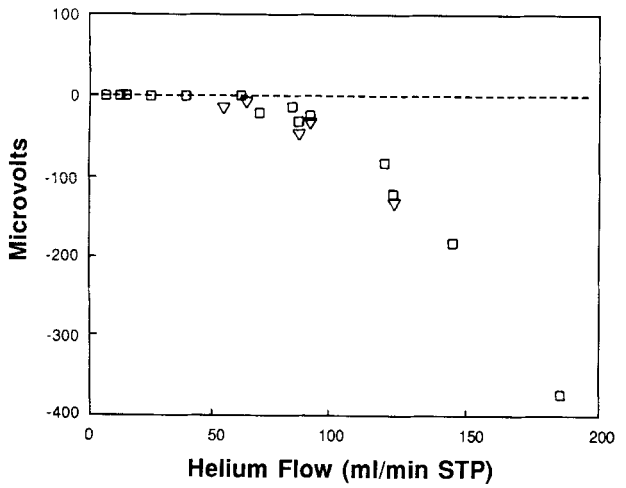


**Figure 2. Bed expansion effects for system A.**

The squares represent flow increases, while the triangles represent flow decreases.

why much higher flow rates could not be studied. Notice that even the smooth time trace of Figure 1a shows a distinct positive spike upon opening the ethane mass flow controller and the downstream ethane shutoff valve. Though the computer simulations have not yet provided an explanation for this phenomenon, it is attributed to the pulse which occurred when pressure waves reached the bed, which apparently caused aggregative movement of the bed. This happened immediately upon increasing the flow, several seconds before the ethane reached the bed.

The interpretation of the observed voltage changes in terms of temperature is essential to the thermometry. It is convenient to write the local, instantaneous solid fraction as

$$\phi(\xi, t) = \Phi(\xi) + \phi'(\xi, t) \tag{10}$$

where $\Phi(\xi)$ is the time average solid fraction at each cross section and the time average of $\phi'(\xi)$ is zero at all $\xi$. As the effect of the fluctuations in solids fraction at a given cross section is averaged out, or removed by filtering, the thermometry can be explained by considering only term III of Eq. 8. The ACP sensitivity $\sigma$ is spatially uniform for the thermometry experiments in this study and $\Gamma$ changes slowly in time relative to the excitation frequency, thus the recorded voltage can be written as

$$V(t_i) = \alpha \int_0^L <\Gamma(\xi, t)>_i \Phi(\xi) d\xi - E_{\text{ref}} \tag{11}$$

where $\alpha$ is a parameter which depends on the operating conditions of the ACP, and $L$ is a constant large enough to include all fluidized material. The time averaging indicated in Eq. 11 was discussed in the Experimental Studies section. Equation 11 has been verified through numerous computer simulations.

If the bed is assumed isothermal, Eq. 11 can be written

$$V(T(t)) = \beta\Gamma(T(t)) - E_{\text{ref}} = a + bT(t) \tag{12}$$

where $\Gamma$ depends only on temperature. The last equation results from assuming that $\Gamma(T)$ is linear in temperature over the limited temperature range studied. As noted in the Experimental Studies section, the ACP voltage is linear in temperature over a limited temperature range. The slope is the experimental voltage sensitivity (calibration) determined for each catalyst and operating condition. The intercept is not of concern since only temperature changes are studied. This eliminates the need to determine absolute moments and minimizes the impact of the slow drift which is characteristic of AC permeameters (Selwood, 1975). Consider the thermometry experiment represented by Figure 1a, which indicates a voltage decrease of 30 $\mu$V upon initiation of ethane hydrogenolysis. The conversion of ethane is 1.4% for this experiment. For the catalyst of system A, with a temperature sensitivity of $-16$ $\mu$V/K, it has been demonstrated that the reproducibility in temperature between experiments at the same conditions is $\pm 0.2$ K. With the indicated sensitivity and after adding in a correction of 3 $\mu$V for the change in hydrogen pressure, the temperature increase of the bed is $2.1 \pm 0.2$ K. This is the increase in the catalyst temperature. The same analysis is applied to all other thermometric experiments. If the temperature is not assumed to be spatially uniform, then Eq. 11 indicates that the recorded voltage is related to the volume average value of $\Gamma$. The thermometry then gives the volume average solid temperature.

It is emphasized that the magnetic thermometry is valid whether or not there are temperature differences between the catalyst particles and the fluid. In a typical experiment involving low ethane conversion, the thermocouple measuring the outlet fluid temperature (at the centerline) indicates an increase to within a few tenths of a degree of the increase in the average catalyst temperature, while the inlet thermocouple increase is considerably lower. The fluid temperatures measured depend somewhat on the exact placement of the thermocouple wells in the presence of reaction (gradients), although their readings were not influenced by their positions for the calibration experiments (no reaction). In addition, these measurements might well be influenced by conduction along the thermocouple wells as well as by the presence of the quartz disk at the inlet. Thus, the magnetic thermometry provides a more reliable measure of reaction temperature than fluid temperature measurements (as made in the experiments described), even if there are no interphase gradients.

## Conclusions

Magnetic crystallite thermometry has been extended to the determination of the volume average catalyst temperature in fluidized beds. The theoretical basis for the thermometry is detailed, with particular focus on explaining why the thermometry is possible in the presence of moving particles. Simulations were used to validate explanations of the resulting voltage vs. time traces. The resulting data are analyzed just as in the established fixed-bed magnetic thermometry, with perhaps some filtering to remove spikes from the voltage vs. time trace. Depending somewhat on the sample moment, the temperature can be determined with a repeatability on the order of a few tenths of a degree. Although experimental configurations to perform the magnetic thermometry may differ between laboratories, the theory behind the thermometry presented here will be useful in the interpretation of thermometry data.

It is difficult to compare the magnetic technique presented

with other available methods. Those methods (Stubington, 1985; Geldart, 1986) measure local solid temperatures and not the bed average solid temperature, unless the bed temperature is assumed spatially uniform. As presented, the magnetic method cannot measure anything but the bed average. No local information is provided. It is also limited by the fact that the detection coils are currently around the reactor. Thus, the method is currently limited to laboratory scale reactors, although any catalyst particle size can be used, according to the theory. The method is also limited to systems which contain superparamagnetic catalysts. Results of general interest can be obtained through modeling.

## Acknowledgment

This work was started with funding from the Petroleum Research Fund and the National Science Foundation.

## Notation

$E$ = instantaneous voltage, $\mu$V
$f$ = primary excitation frequency, Hz
$H$ = magnetic field strength, Oe
$I$ = magnetization, Oe
$k$ = Boltzmann's constant, erg/K
$L$ = integration length, maximum bed height, cm
$M$ = magnetization, Oe
$t$ = time, s
$T$ = temperature, K
$\langle v \rangle$ = average nickel crystallite volume, cm$^3$
$V$ = time averaged RMS voltage recorded, $\mu$V

### *Greek letters*

$\xi$ = position coordinate in coil, cm
$\sigma$ = ACP sample sensitivity, $\mu$V/Oe/s
$\Gamma$ = temperature dependence of low field moment
$\phi$ = fraction of cross section which is catalyst
$\Phi$ = time-average solid fraction at each cross section
$\psi$ = fraction of the solid which is nickel
$\beta$ = defined by Eq. 12
$\omega$ = excitation voltage frequency, rad

## Literature Cited

Arnaldos, J., M. Lazaro, and J. Casal, "The Effect of Magnetic Stabilization on the Thermal Behavior of Fluidized Beds," *Chem. Eng. Sci.*, **42**(6), 1501 (1987).
Cale, T. S., "Nickel Crystallite Thermometry During Ethane Hydrogenolysis," *J. Cat.*, **90**(1), 40 (1984).
Cale, T. S., "Effectiveness Factor for a Single Pellet During Ethane Hydrogenolysis," *Chem. Eng. Comm.*, **70**, 57 (1988).
Cale, T. S., and J. M. Lawson, "Application of Catalytic Crystallite Thermometry to Interphase Transport Studies," *Chem. Eng. Comm.*, **39**, 241 (1985).
Cale, T. S., J. M. Lawson, and D. K. Ludlow, "Low Re Interphase Nu for Axial Dispersion and Bypassing Reactor Models," *Chem. Eng. Comm.*, **56**, 169 (1987).
Cale, T. S., and D. K. Ludlow, "Magnetic Crystallite Thermometry," *J. Cat.*, **86**(2), 450 (1984a).
Cale, T. S., and D. K. Ludlow, "Application of AC Permeametry to Catalytic Crystallite Thermometry," *Anal. Inst.*, **13**(2), 183 (1984b).
Cale, T. S., and J. A. Merson, "Magnetic Determination of Axial Catalyst Temperature Profiles," *AIChE J.*, **35**(9), 1428 (1989).
Geldart, D., ed., *Gas Fluidization Technology*, John Wiley, New York (1986).
Hudgins, R. R., "Inadequacy of Criteria for Detecting Interphase Transport Intrusions," *Chem. Eng. Sci.*, **36**(9), 1579 (1981).
Holstein, W. L., and M. Boudart, "The Temperature Difference Between a Supported Catalyst Particle and its Support During Exothermic and Endothermic Catalytic Reactions," *Rev. Latinoam. Ing. Quim. Quim. Apl.*, **13**(2), 107 (1983).
Kunii, D., and O. Levenspiel, *Fluidization Engineering*, John Wiley, New York (1969).
Ludlow, D. K., "The Application of Magnetic Crystallite Thermometry to Low Reynolds Number Interphase Heat Transfer," PhD Diss., Arizona State Univ. (1986).
Luss, D., "Temperature Rise of Catalytic Supported Crystallites," *Chem. Eng. J.*, **1**(4), 331 (1970).
Rosensweig, R. E., *Ferrohydrodynamics*, Cambridge University Press, Cambridge (1985).
Selwood, P. W., *Chemisorption and Magnetization*, Academic Press, New York (1975).
Stubington, J. F., "Comparison of Techniques for Measuring the Temperature of Char Particles Burning in a Fluidized Bed," *Chem. Eng. Res. Des.*, **63**, 241 (1985).

*Manuscript received Dec. 13, 1991, and revision received May 8, 1992.*